

Inverse Model Based Torque Vectoring Control For a Rear Wheel Driven Battery Electric Vehicle

T. Bunte* S. Kaspar** S. Hohmann*** J. Brembeck*

* *Institute of System Dynamics and Control, DLR Oberpfaffenhofen, Germany (e-mail: {Tilman.Buente, Jonathan.Brembeck}@dlr.de).*
** *BMW Group, Munich, Germany (e-mail: Stephan.Kaspar@bmw.de)*
*** *Karlsruhe Institute of Technology, Karlsruhe, Germany (e-mail: soeren.hohmann@kit.edu)*

Abstract: This paper presents the torque vectoring control concept for a vehicle with two powerful wheel individual electric drives at the rear axle. The direct yaw moment control which is enabled by the torque difference offers the potential for shaping the vehicle's yaw dynamics in a considerable range. The control concept introduced here is primarily oriented at the practical target of demonstrating the potential of the prototype vehicle's innovative rear axle. Nevertheless, together with the tools presented here it is conveniently adaptable to any vehicle data. The focus is on yaw dynamics control. A reference yaw rate is determined by combining conveniently tunable linear dynamics with a nonlinear steady state gain, the latter in order to establish a desired self-steering behavior. In order to reshape the yaw response after steering inputs an inverse single track model is used as a significant part of the applied feed-forward control. Moreover, the same inverse model is employed by the optional yaw rate feedback control which is based on the inverse disturbance observer scheme. Both the effectiveness of the control concept and the practical ease of control parameter tuning were validated in driving experiments.

1. INTRODUCTION

Up to now, battery electric vehicles have mostly been developed according to the conversion design principle. That means that the vehicle is designed as a version of a series car which was otherwise devised for being propelled by an internal combustion engine. However, how can an electric car be constructed without making this compromise but trying to shift as much as possible from the drive train into the wheel? This problem was investigated in a research project FAIR (Fahrwerk/Antrieb-Integration ins Rad, transl. chassis/drive integration into the wheel) under the lead of BMW Group Forschung und Technik together with its partners Schaeffler and German Aerospace Center (DLR). This paper deals with the torque vectoring control applied to the electrically propelled rear axle of the FAIR demonstrator vehicle. The issue of torque vectoring control has been addressed by quite a number of articles. In Pruckner et al. (2011) fundamental considerations showed the benefit of torque vectoring for a vehicle with tail-heavy mass distribution. Already classical PID yaw rate feedback while imposing heuristic bounds on both yaw rate and vehicle side slip can yield enhanced handling and driving dynamics, Pinto et al. (2010). Similarly to our approach, in He et al. (2005) and Kaspar et al. (2013) inverse model based feed forward control is combined with yaw rate feedback. Also, a scalable single track model is employed to generate the reference yaw dynamics. In Canale et al. (2007) and Canale et al. (2008) IMC based control and a sliding mode controller respectively are applied for robust yaw control of a vehicle with an active differential. One

goal there is improvement of vehicle handling in terms of implementing both a desired steady state understeering characteristics and a target transient response. Another approach which has been used in manifold publications is LQR-based direct yaw moment control, Esmailzadeh et al. (2003), Geng et al. (2009). However, for experimentally validated torque vectoring control the disclosure of details in the literature is still rare. With our paper we present the reproducible combination of some above mentioned torque vectoring feed-forward features with the so-called inverse disturbance observer, an efficient and easy-to-tune control scheme, Bajcinca and Bunte (2005), which ideally amends the feed-forward function blocks. Driving experiments on both dry asphalt and a frozen lake in Lapland proved good stability and handling of the vehicle controlled in such a way.

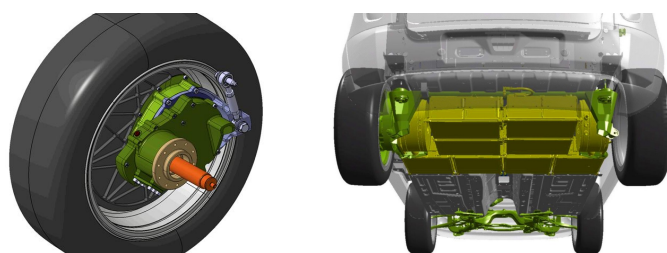


Fig. 1. Innovative rear wheel gear train assembly also serving as wheel guidance and suspension (el. motor omitted, left). Experimental vehicle with mechatronic rear axle (view from below, right).

The paper is organized as follows. Section 2 briefly describes the mechanic properties and equipment of the experimental vehicle. After that, section 3 introduces the torque vectoring concept for both longitudinal control and yaw dynamics control including implementational aspects. Before some concluding remarks, experimental validation is presented in section 4.

2. MECHATRONIC AXLE AND EXPERIMENTAL VEHICLE

The goal of the FAIR project was the systemic investigation of so-called in-wheel-variants where chassis and drive train components are integrated into the wheel. Various concepts were designed and virtually assessed before the most promising was chosen, optimized, and put into prototype hardware in terms of a mechatronic rear axle, Pruckner (2011). It turned out that despite the purpose design approach, a modified series car was suitable as carcass for a drivable demonstrator. It was realized by BMW based on a MINI Countryman series car. Therefore, the internal combustion engine and the conventional rear axle including friction brakes were completely removed, though keeping the conventional hydraulic brake system at the front axle. The replacing electric rear axle allows for complete energy recuperation during moderate braking. The battery is mounted under the trunk hardly visible between the wheels of the rear axle (see Fig. 1, right). This compact design is serviceable for a low center of gravity and for crash safety of the high-voltage battery. Moreover, there is no reduction of the available seats. This has become feasible by the main innovation achieved by the FAIR project: A novel gear train assembly combines the basic chassis functions propulsion, wheel guidance, and suspension (see Fig. 1, left). Moreover, it enables mounting of the electric drives to the vehicle body without any bulky articulated shafts. By means of the two rear wheel individual electric motors the driving behavior can be designed by software in a wide range and in a highly dynamic manner. Thus, vehicle dynamics handicaps due to the unfavorable battery location induced load shift towards the rear axle can be compensated. The demonstrator is extensively equipped with measurement equipment such as inertial measurement unit and optical velocity sensor and allowed for conclusive experimental validation of the mechatronic axle. Together with the DLR-Institute of System Dynamics and Control, the vehicle was successfully tested in driving experiments on BMW test tracks in Germany and Sweden using the torque vectoring control presented in this paper.

3. TORQUE VECTORING CONTROL CONCEPT

The aim of the torque vectoring control concept described here was to reveal the vehicle dynamics potential of the demonstrator vehicle featuring the mechatronic rear axle. Direct application to series cars was not intended and therefore, specific robustness requirements w.r.t. varying operating conditions (esp. changes in the road tire friction coefficient) were not given. Nevertheless, a robustness analysis of the controlled vehicle was undertaken in a separate activity, Kaspar et al. (2014). The control concept uses the motor torque set points as control variables to

implement both desired longitudinal and yaw dynamics of the vehicle corresponding to a reference dynamics. The total control structure is depicted in Fig. 2. The driver directly operates the front wheel steering angle δ_f via the steering wheel angle δ_{SW} and the front axle brake pressure by the brake pedal position BP . The rear axle wheels are propelled by electric motors applying the torques τ_l and τ_r at the left and right hand side, respectively. Drive torques are positive and braking (recuperative) torques have negative sign. From all wheel speeds the total vehicle speed v is estimated and used for scheduling of the filters where suitable. The measured yaw rate $\dot{\psi}$ can be used for feedback control. Additional measurement signals are the lateral acceleration a_y and the chassis side slip angle β both effective at the center of gravity. The torque vectoring control uses superposition of the rear axle mean drive torque $\bar{\tau} = (\tau_r + \tau_l)/2$ and a term $\Delta\tau/2 = (\tau_r - \tau_l)/2$ with positive sign at the right wheel and negative sign at the left wheel, respectively. The mean drive torque is responsible for the longitudinal motion of the car. The torque difference $\Delta\tau$ between right and left wheel causes a yaw torque (denoted ΔM_z in the controller internal representation) which acts on the car body additionally to the yaw torque which is induced by the lateral tire forces. The gain between $\Delta\tau$ and ΔM_z depends on the radius r_w of the wheels and the rear axle track width w . Thus, using the signal ΔM_z in Fig. 2 the yaw motion of the vehicle can effectively be influenced in terms of both yaw rate feed-forward and feedback control. This will be explained in section 3.2. Other auxiliary control functions are explained in section 3.3.

3.1 Longitudinal dynamics feed-forward control

The set point of the longitudinal force F_x to be acting on the vehicle by virtue of the rear axle is calculated based on both accelerator AP and brake pedal BP positions. Non-linear characteristics are used to apply a pedal-dependent portion of the actually available maximum torques. These depend on the driving state (i.e. the vehicle speed) and reflect the limitations both on motor torque and power. For the operational case of braking, the brake force distribution between the hydraulically braked front axle and the electric rear axle is chosen such that recuperation is maximized to yield good efficiency. However, lateral vehicle stability limits are considered at any time. At small accelerator pedal positions, the characteristics is designed to induce a speed dependent drag moment. Thus, the driver can conveniently handle moderate decelerations without the need to change over his foot to the brake pedal. During driving experiments it turned out that the characteristics which had been tuned by means of preceding simulations needed only little adaptation in order to have a well drivable car. Details of the longitudinal control are omitted here since our focus here is rather on lateral and yaw dynamics.

3.2 Yaw dynamics control

The yaw dynamics of the vehicle can be affected by setting a torque difference $\Delta\tau$ at the rear axle, cf. Fig. 2. As long as the torque difference is zero the vehicle exhibits what we here call its *natural yaw dynamics*. The lateral and yaw

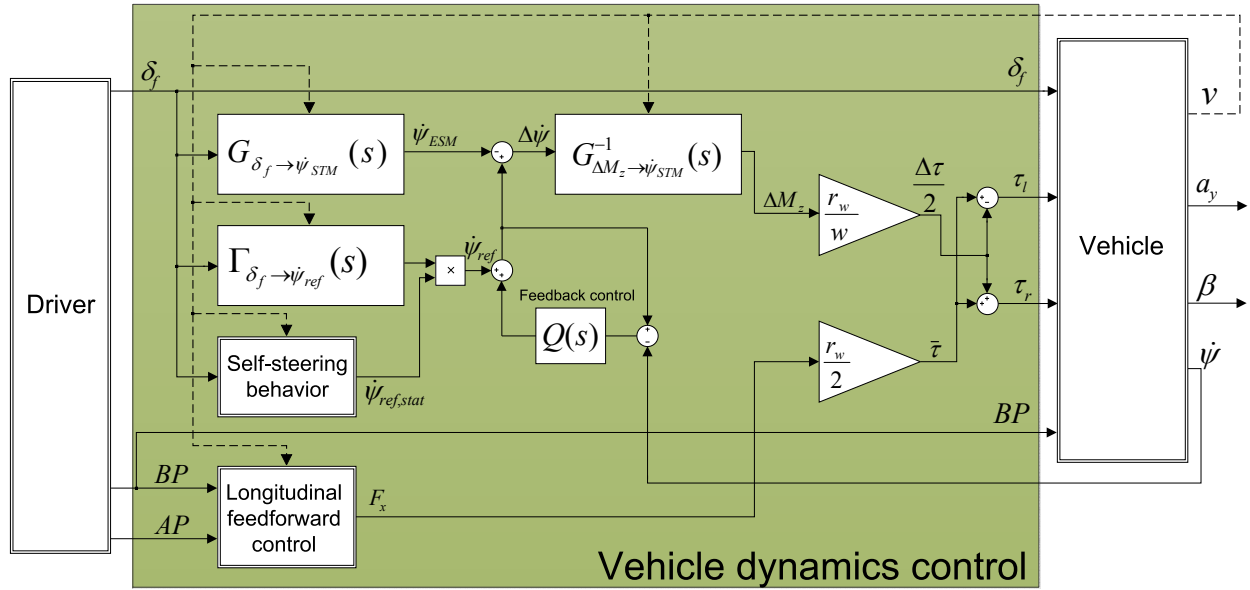


Fig. 2. Torque vectoring control structure

dynamics of a vehicle up to moderate lateral accelerations (4 m/s² on dry road) can be described by the well-known single track model. We employ this second order linear model for control synthesis while using the notation from Ackermann et al. (2002). The correctly parameterized single track model of the vehicle's natural yaw dynamics is denoted with *STM*. It plays a significant role for the cancelation of the vehicle's uncontrolled yaw dynamics in the torque vectoring control concept. The transfer function

$$G_{\delta_f \rightarrow \dot{\psi}_{STM}}(s) = \frac{\dot{\psi}_{STM}(s)}{\delta_f(s)} \quad (1)$$

describes the single track model relation between the front steering angle δ_f and yaw rate $\dot{\psi}$.

Inverse model based cancelation of vehicle yaw dynamics
The transfer function

$$G_{\Delta M_z \rightarrow \dot{\psi}_{STM}}(s) = \frac{\dot{\psi}_{STM}(s)}{\Delta M_z(s)} \quad (2)$$

describes the single track model relation between the additional yaw moment ΔM_z and the vehicle's yaw rate. It has one zero in the left half plane and a relative degree of one. After adding an extra sufficiently fast zero on the negative real axis, it can be inverted to a stable transfer function $\tilde{G}_{\Delta M_z \rightarrow \dot{\psi}_{STM}}^{-1}(s)$ as a good approximation. Using feed-forward control

$$\Delta M_z(s) = -\frac{G_{\delta_f \rightarrow \dot{\psi}_{STM}}(s)}{\tilde{G}_{\Delta M_z \rightarrow \dot{\psi}_{STM}}^{-1}(s)} \delta_f(s) \quad (3)$$

as shown in Fig. 2 the natural yaw dynamics can approximately be canceled similarly to He et al. (2005), Canale et al. (2007, 2008). If $\dot{\psi}_{ref} = 0$ is imagined in Fig. 2 and no feedback is assumed (i.e. $Q(s) = 0$) then the torque difference $\Delta \tau$ would be computed such that the vehicle's yaw reaction completely resists any driver input at the steering wheel. Evidently, this holds only depending on the validity of the employed single track model and when assuming ideal actuators.

Reference yaw dynamics design Apparently, for a well drivable vehicle it should rather follow an appropriate reference yaw rate $\dot{\psi}_{ref}$. Since the natural yaw dynamics is compensated for as described above, the vehicle's yaw response to steering wheel inputs could be designed arbitrarily by means of the reference yaw rate. However, this is true only from the viewpoint of linear theory. In practice, it should be regarded that the yaw dynamics is not deformed too forcibly away from the natural dynamics. Otherwise, during heavy maneuvers there is evident risk of overloading the motors, power converters, and gears.

Moreover, nonlinear effects like saturation of motor torques or tire forces will restrain the desired performance but lead to an unbalanced, rude, or noisy driving behavior instead. This fact was clearly confirmed during our driving tests when using extreme parameterization of the reference yaw dynamics. As a part of our concept concerning reference yaw dynamics, we divided it into a static and a dynamic factor. That way, a desired nonlinear steady state self-steering behavior can be combined with linear dynamics as already shown in Kaspar et al. (2012). Consequently, the reference yaw rate $\dot{\psi}_{ref}$ is composed of the steady state value $\dot{\psi}_{ref,stat}$ and a dynamic part with unity steady state gain.

Steady state self-steering characteristics The steady state value $\dot{\psi}_{ref,stat}$ is calculated by means of a function block depending on the vehicle speed v and the steering angle δ_f . The calculation is targeted on the realization of a desired self-steering behavior, Canale et al. (2007), which can be parameterized arbitrarily within bounds during application. In particular, it is possible to implement nonlinear (e.g. progressive) self-steering characteristics by defining the coefficients of a corresponding polynomial. Note that in this case the functional implementation requires the determination of polynomial roots in every discrete execution cycle. *Self-steering behavior* denotes the change of the steering angle demand being necessary in a quasi

steady state driving experiment to stay on a circle with constant radius while the speed is slowly increased. The resulting steering angle usually is plotted over the lateral acceleration. The *self-steering gradient SSG* is the slope of this curve. On the left side of Fig. 3 the natural self-steering behavior of the experimental car is depicted with a black solid line. In this diagram, it refers to the steering wheel angle

$$\delta_{SW} = i_s \cdot \delta_f \quad (4)$$

where i_s is the steering gear ratio. The fluctuation of δ_{SW} is caused by the test driver's control action for staying on the circle. Hence, only the trend is relevant. The dashed black line represents the self-steering behavior of the *STM* model and matches well the real car. Up to 6 m/s^2 lateral acceleration there is no recognizable nonlinear deviation. The torque difference $\Delta\tau$ is zero (see right) for the natural (i.e. uncontrolled) vehicle. In our experiments we restricted the investigation of self-steering behavior to linear variants (i.e. each with constant self-steering gradient). The calculation of the steady state reference yaw rate $\dot{\psi}_{ref,stat}$ uses the following relation which holds in steady state and where R is the actual curve radius:

$$a_y = v \cdot \dot{\psi} = v^2/R \quad (5)$$

The desired self-steering characteristics $\Delta\delta_{SW}(a_y)$ is defined by

$$\delta_{SW} = i_s \cdot \ell/R + \Delta\delta_{SW}(a_y) \quad (6)$$

where ℓ is the vehicle's wheel base. In the case of linear characteristics (6) becomes

$$\delta_{SW} = i_s \cdot \ell/R + SSG_{SW} \cdot a_y \quad (7)$$

with the self-steering gradient SSG_{SW} (cf. dashed lines in Fig. 3, left). Generally, in the functional block *Self-steering behavior* in Fig. 2 the nonlinear set of equations (4) - (6) needs to be solved. In case of linear self-steering characteristics the rule for calculation of the steady state reference yaw rate simplifies to

$$\dot{\psi}_{ref,stat} = \frac{v}{\ell + SSG_{SW}/i_s \cdot v^2} \delta_f \quad (8)$$

Besides natural under-steering behavior (black line in Fig. 3) we also tested neutral steering (green), over-steering (blue), and sharp under-steering (red). The corresponding self-steering gradient values used to define the desired self-steering behavior are shown with the legend

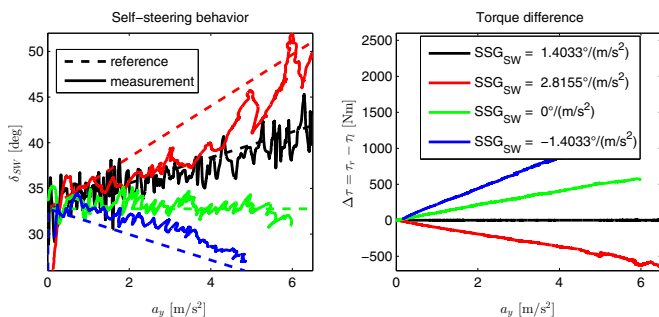


Fig. 3. Riding on a circle with radius $R = 71 \text{ m}$: Experimental comparison of self-steering behaviors as implemented by means of different desired self-steering gradients (left). Corresponding rear wheel torque differences $\Delta\tau$ (right).

on the right side of Fig. 3. The plots in this figure display the torque differences $\Delta\tau$ which result from the steady state feed-forward control as described above. No feedback action is used so far ($Q(s) = 0$) and the steady state gain of the dynamic filter $\Gamma_{\delta_f \rightarrow \dot{\psi}_{ref}}(s)$ is unity (see next paragraph). As a result of the experiments it can be stated that the self-steering behavior can be significantly modified using rear axle torque vectoring. Moreover, specific desired self-steering characteristics may be implemented quite precisely by means of mere feed-forward control. However, large deviations from the vehicle's natural behavior demand for large torque differences $\Delta\tau$. Therefore, with limited motor torques, in practice the range of self-steering behavior adaptations is also limited.

Linear reference yaw dynamics The dynamic behavior of the reference yaw rate $\dot{\psi}_{ref}$ is determined by the linear filter

$$\Gamma_{\delta_f \rightarrow \dot{\psi}_{ref}}(s) = \frac{G_{\delta_f \rightarrow \dot{\psi}_{ref}}(s)}{G_{\delta_f \rightarrow \dot{\psi}_{ref}}(0)} \quad (9)$$

By virtue of the denominator the steady state gain of this filter is normalized to unity. This corresponds to the notion that the steady state behavior is solely determined by the desired self-steering behavior as described above. In principle the time response of the reference yaw signal after a steering wheel angle step input can be chosen arbitrarily. But again, the deviation from the vehicle's natural behavior should be constrained in order to avoid nonlinear effects and to reduce power consumption as well as wear and tear. Therefore, a single track model is employed again. Here, it facilitates targeted response modification starting from the natural yaw dynamics. The following three step approach is suggested:

- Firstly, the transfer function $G_{\delta_f \rightarrow \dot{\psi}_{ref}}(s)$ is chosen identical with $G_{\delta_f \rightarrow \dot{\psi}_{STM}}(s)$ thus approximately matching the vehicle's natural yaw dynamics.
- In the second step the physical parameters of the reference single track model can be adapted according to one's wishes. For example the yaw moment of inertia $J_{z,ref}$ can be reduced versus $J_{z,STM}$ to give the vehicle a better agility. The resulting transfer function can be represented in the following form, He et al. (2005)

$$G_{\delta_f \rightarrow \dot{\psi}_{STM,mod}}(s) = \frac{K(v) (1 + T(v)s)}{1 + 2D(v) \frac{s}{\omega_D(v)} + \left(\frac{s}{\omega_D(v)} \right)^2} \quad (10)$$

Here, $K(v) = G_{\delta_f \rightarrow \dot{\psi}_{STM,mod}}(0)$ is a symbol representing the steady state gain, $D(v)$ is the damping ratio of the eigenvalues, $\omega_D(v)$ denotes the natural frequency of the eigenvalues, and $T(v)$ is the derivative time associated with the zero. The formulas for these speed dependent parameters are skipped here since they can straightforwardly be derived from the single track model (see, e.g. Ackermann et al. (2002)).

- Finally, in step three the speed dependent parameters of the transfer function $G_{\delta_f \rightarrow \dot{\psi}_{STM,mod}}(s)$ are modified

further to form the final reference yaw dynamics transfer function:

$$G_{\delta_f \rightarrow \dot{\psi}_{ref}}(s) = \frac{\lambda_K K(v) \left(1 + \frac{T(v)s}{\lambda_Z \lambda_s}\right)}{1 + 2(1 - \lambda_D(1 - D(v))) \frac{s}{\lambda_s \omega_D(v)} \left(\frac{s}{\lambda_s \omega_D(v)}\right)^2} \quad (11)$$

With the new dedicated parameters λ_K , λ_D , λ_s , and λ_Z the dynamics properties can be individually adapted. For each, a value of one means no modification.

λ_D modifies the damping ratio. Variation of λ_D in the range $0 \dots 1$ changes the resulting damping ratio between unity and D . This parameter can be used to give the steering response a better damping.

λ_Z modifies the significance of the transfer function zero. A higher value increases derivative action. Therefore, this parameter is specifically suitable to enhance the dynamic responsiveness of the vehicle to steering wheel inputs.

λ_s causes a scaling in time. The transient steering response executes λ_s -times faster.

λ_K scales the steady state gain. In the context of the specific control concept presented here, this parameter is not used further (i.e. we use $\lambda_K = 1$), because the steady state reference yaw rate is supposed to be uniquely determined by the desired self-steering behavior.

A remarkable property of the described parameterization of the reference yaw dynamics is that it is relative to the natural behavior of the car for all vehicle speeds. This corresponds to the already explained concept of changing the properties only moderately in order not to evoke saturation effects. Note that steps two and three are optional and the application engineer can decide if a tuning of single track parameters is more suitable or tuning the λ -parameters or a combination of both. By virtue of the comprehensible meaning of all parameters, the tuning during application of the torque vectoring control is fairly easy and convenient. In our experiments we found, that for the demonstrator vehicle the agility could be noticeably improved by choosing $\lambda_Z > 1$. At the same time, setting $\lambda_D < 1$ helped to give the car a good driveability. In contrast, changing λ_s did not bring handling benefits.

To facilitate the tuning by an application engineer and to illustrate the effects of λ -parameter changes it appears useful to have a suitable tool, which can as well support on-line parameterization during application. Fig. 4 shows a number of screen shots of such a Matlab-GUI based tool. Given a set of single track parameters corresponding to (10) the λ -parameters in (11) can be modified by means of sliders and the changed yaw rate response (green line) to a steering step input can immediately be compared to that of the unmodified single track model (red lines). The top slider facilitates the change of the vehicle speed such that the result of the current parameterization can conveniently be observed over the entire operational speed range. Once the parameterization is chosen, the λ -parameters can be downloaded to the rapid control prototyping hardware for

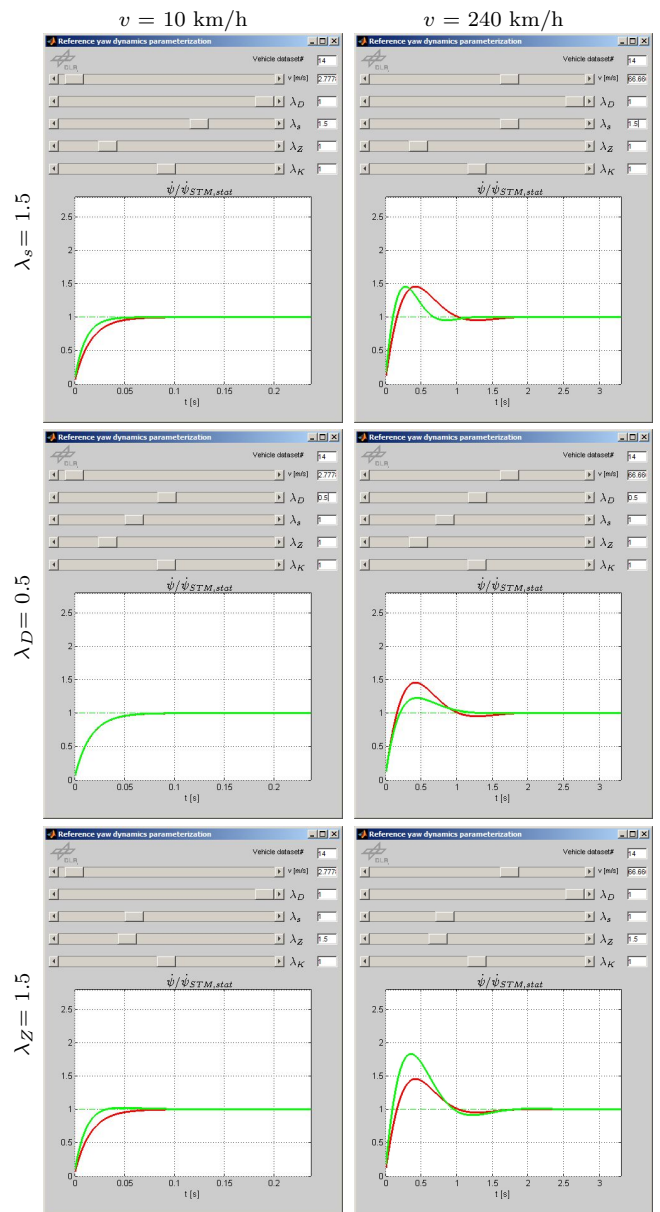


Fig. 4. Application tool for reference yaw dynamics tuning updating the parameters of the filter (9) as implemented in the controller code.

Yaw rate feedback Yaw rate feedback can be used to improve the fidelity of the vehicle's dynamic response w.r.t. the reference yaw rate. Moreover, the car is stabilized when external disturbances occur. We adopted the Inverse Disturbance Observer (IDOB) control structure, Bajcinca and Bunte (2005), because of its effectiveness and ease

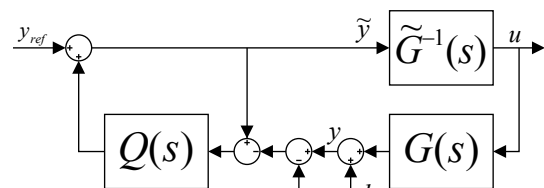


Fig. 5. Generic IDOB control structure

of practical application. The IDOB scheme (cf. Fig. 5) can be seamlessly combined with the already introduced feed-forward control structure due to the presence of the inverse model according to the denominator in (3). The IDOB control scheme is quickly explained based on the following linear considerations. Therefore, assume that i) the cancelation of the vehicle's yaw response to mechanical steering δ_f inputs by means of (3) is accurate and ii) $Q(s)$ is a unity gain low pass filter. The following transfer matrix

$$\dot{\psi}(s) = \frac{\begin{bmatrix} G_{\Delta M_z \rightarrow \dot{\psi}_{veh}}(s) & 1 - Q(s) \\ \tilde{G}_{\Delta M_z \rightarrow \dot{\psi}_{STM}}(s) & \end{bmatrix}}{1 - Q(s) \left(1 - \frac{G_{\Delta M_z \rightarrow \dot{\psi}_{veh}}(s)}{\tilde{G}_{\Delta M_z \rightarrow \dot{\psi}_{STM}}(s)} \right)} \begin{bmatrix} \dot{\psi}_{ref}(s) \\ d(s) \end{bmatrix} \quad (12)$$

which can be derived from Fig. 5 while using the following equivalences compared to Fig. 2: $y_{ref} = \dot{\psi}_{ref}$, $u = \Delta M_z$, $y = \dot{\psi}$, $G(s) = G_{\Delta M_z \rightarrow \dot{\psi}_{veh}}(s)$ representing the vehicle, and $\tilde{G}(s) = \tilde{G}_{\Delta M_z \rightarrow \dot{\psi}_{STM}}(s)$. Eq. (12) shows the effect of the reference yaw rate $\dot{\psi}_{ref}$ and an external disturbance d on the yaw rate response of the torque vectoring controlled vehicle. From (12) it can be easily concluded that for frequencies below the bandwidth of the Q -filter (i.e. where $Q \approx 1$) the yaw rate follows the reference value $\dot{\psi}(s)/\dot{\psi}_{ref}(s) \approx 1$ and disturbances are attenuated $\dot{\psi}(s)/d(s) \approx 0$. Obviously, good accuracy of the inverted plant model i.e. $G_{\Delta M_z \rightarrow \dot{\psi}_{veh}}(s)/\tilde{G}_{\Delta M_z \rightarrow \dot{\psi}_{STM}}(s) \approx 1$ contributes to favorable control performance. Detailed analysis and further properties of the IDOB control structure like stability and general robustness issues can be found in Bajcinca and Bunte (2005). Note that in practice a major benefit from using the proposed IDOB structure for yaw rate feedback is the ease of tuning:

- The inverse single track model used should apparently be parameterized to best fit the real vehicle. Scheduling with speed is mandatory. If further actual parameter estimates are available e.g. for load mass or road/tire friction coefficient, on-line model parameter adaption may be appropriate to improve robustness. In our driving experiments (see section 4), we tuned the road/tire friction coefficient of the single track model to adapt to the conditions (dry road vs. frozen lake surface).
- Another tunable parameter is the zero added to $\tilde{G}_{\Delta M_z \rightarrow \dot{\psi}_{STM}}(s)$ to enable inversion. This zero should be chosen as fast as the controller sampling rate permits.
- The main IDOB tuning is required for the bandwidth of the unity gain Q -filter. If a first order low pass filter is chosen, only the time constant needs to be set. Tuning can be accomplished conveniently with a couple of driving experiments starting with low Q -filter bandwidth. When stepwise increasing the bandwidth approaching the stability limit of the controlled system can normally be clearly observed in terms of unbalanced oscillatory driving behavior. Nevertheless, scientifically based tuning and a robust stability proof are readily available, (Bajcinca and Bunte (2005)).

Robustness of our specific yaw rate feedback control scheme is thoroughly investigated in a separate work, Kaspar et al. (2014), using the parameter space method, Ackermann et al. (2002). In driving experiments, the effectiveness of the feedback scheme was proven (see section 4).

3.3 Controller implementation

On the experimental car, the torque vectoring controller according to Fig. 2 was implemented using Matlab/Simulink and a dSPACE Autobox with corresponding rapid control prototyping tool chain. All transfer functions were realized in controllable canonical state space representation as Embedded Matlab functions. This implementation supports time variability of parameters (speed of single track model in particular). For the practical implementation a number of issues needed to be tackled among which are the following. Firstly, anti-windup of the controller is necessary. In general, the IDOB control scheme exhibits high gain integral action which is comprehensible from analysis of the open loop transfer function (cut at y) in Fig. 5. However, saturation of the actuators or the tire forces may cause that the desired yaw rate $\dot{\psi}_{ref}$ is physically not feasible. Without counteraction this would result in integral windup. Our remedy uses detection of tire force saturation. Tire slip is then bounded by a simple degressive characteristic which reduces the motor torque magnitudes as soon as one of the rear axle wheel slips exceeds the estimated value belonging to maximum tire force. This heuristic approach works sufficiently well when the tire slips are known which was the case in our well instrumented testing car. Hence, no sophisticated wheel slip control was necessary for wheel slip control was not in the focus of this work. The gain reduction associated with the resulting torque difference $\Delta\tau$ degradation can be used to reduce the gain of the Q -filter by the same quota. The same strategy is used in case of saturation of the motor torques or the battery power: The resulting gain reduction of (2) relating to the real car is considered by a reduction of the Q -filter gain of the same magnitude. This action removes integral behavior of the Q -loop and thus avoids control windup. Finally, agile torque vectoring control implies quick reversing of the motor torques. The resulting load shocks (Ferraria effect) may cause impairment to the motor gears and acoustic interference. Therefore, damping of Ferraria effect was implemented by means of rate limitation of the motor torque set-points. Good trade-off between dynamic performance and load shock damping was realized by making torque rate limitation only effective near the reversing juncture. This was realized by scheduling the motor torque set-point rate limits with the actual torque magnitude.

4. DRIVING EXPERIMENTS

Driving experiments were conducted both on dry asphalt and on a frozen lake to investigate performance of the electrically driven rear axle and the control concept under diverse operating conditions. It should be noted that the project focus was on demonstrating the vehicle dynamics potential of the novel electric rear axle. Therefore, adaptation to parameter variations other than speed had not explicitly been addressed in the control design. Thus,

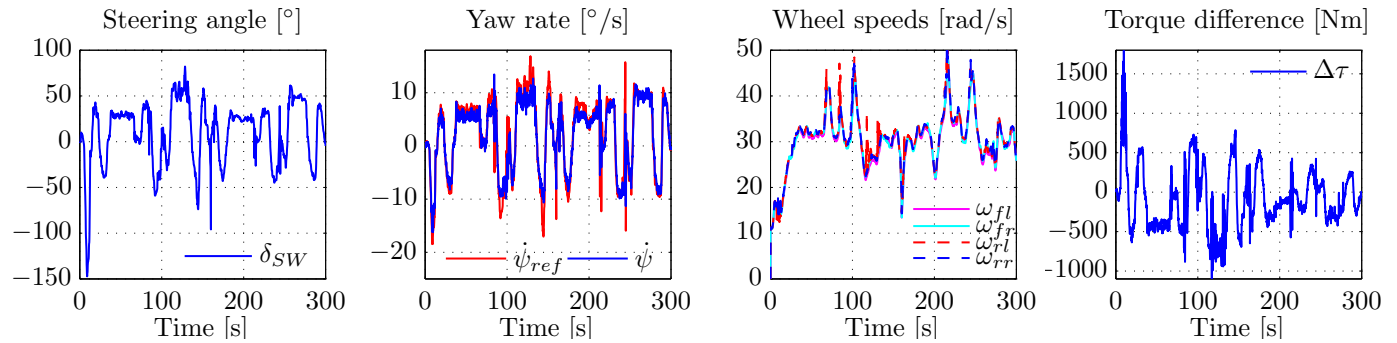


Fig. 6. Experimental torque controller evaluation on the handling course on a frozen lake in Lapland.

the road/tire friction coefficient assumed in the controller was adapted manually to the operating conditions. Both campaigns obtained good results. A small sequence from driving on a very low friction handling course is shown in Fig. 6. Despite maneuvering at the friction limits, the yaw rate remains stable and follows well the set point. The yaw dynamics appears well damped (upper left plot). Subjective assessment confirmed the good controllability of the car. Occasionally, the left rear wheel exhibits increased slip (red dashed line in third plot from left) while accelerating in left turns. This however, is quickly recaptured by means of the heuristic slip control.

5. CONCLUSION

An easy implementable and straight forward torque vectoring control structure was developed. Good performance was proven in a wide range of operating conditions. Experimental assessment both on dry asphalt and on a frozen lake surface confirmed extra-ordinary stability of the controlled vehicle. On this occasion, also the suitability of the various concepts and modules presented in this paper was validated such as the composition of separately designed steady state and dynamical yaw rate set points, inverse model based yaw dynamics cancelation, inverse disturbance observer based yaw rate feedback, and the proposed anti-windup concept. Both the feed-forward and the feedback control modules are model based and easy to tune. Robustness analysis by means of the parameter space method was worked out after completion of the project, Kaspar et al. (2014).

ACKNOWLEDGEMENTS

The FAIR project received financial support by Bayerische Forschungsförderung (grant AZ-840-08, cf. Leonhardt (2013)).

REFERENCES

- Ackermann, J., Blue, P., Bünte, T., Güvenc, L., Kaesbauer, D., Kordt, M., Muhler, M., and Odenthal, D. (2002). *Robust Control: The Parameter Space Approach*. Springer, London.
- Bajcinca, N. and Bünte, T. (2005). A novel control structure for dynamic inversion and tracking tasks. In *Proc. 16th IFAC World Congress*. Prague.
- Canale, M., Fagiano, L., Ferrara, A., and Vecchio, C. (2008). Vehicle yaw control via second-order sliding-mode technique. *Industrial Electronics, IEEE Transactions on*, 55(11), 3908–3916.
- Canale, M., Fagiano, L., Milanese, M., and Borodani, P. (2007). Robust vehicle yaw control using an active differential and IMC techniques. *Control Engineering Practice*, 15(8), 923 – 941.
- Esmailzadeh, E., Goodarzi, A., and Vossoughi, G. (2003). Optimal yaw moment control law for improved vehicle handling. *Mechatronics*, 13(7), 659–675.
- Geng, C., Mostefai, L., Denai, M., and Hori, Y. (2009). Direct yaw-moment control of an in-wheel-motored electric vehicle based on body slip angle fuzzy observer. *Industrial Electronics, IEEE Transactions on*, 56(5), 1411–1419.
- He, P., Hori, Y., Kamachi, M., Walters, K., and Yoshida, H. (2005). Future motion control to be realized by in-wheel motored electric vehicle. In *Industrial Electronics Society, 2005. IECON 2005. 31st Annual Conference of IEEE*.
- Kaspar, S., Ludwig, J., Bünte, T., and Hohmann, S. (2014). Robust torque vectoring control. In *19th IFAC World Congress*. Cape Town.
- Kaspar, S., Pruckner, A., and Stroph, R. (2012). Potential of vehicle dynamics via single wheel drive for installation space optimized electric vehicles. In *Proc. 21. Aachener Kolloquium Fahrzeug- und Motorentechnik*. Aachen.
- Kaspar, S., Stroph, R., Bünte, T., and Hohmann, S. (2013). Fahrdynamikoptimierung mittels Torque Vectoring bei einem bauraumoptimierten Elektrofahrzeug. *Automobiltechnische Zeitschrift (ATZ)*, 116(2), 72–78.
- Leonhardt, D. (ed.) (2013). *Jahresbericht 2012*. Bayerische Forschungsförderung.
- Pinto, L., Aldworth, S., M. Watkinson, Jeary, P., and Franco-Jorge, M. (2010). Advanced yaw motion control of a hybrid vehicle using twin rear electric motors. In *Proceedings of AVEC 2010*, pp. 640–645. Loughborough, UK.
- Pruckner, A. (2011). Potentiale eines radnahen Elektroantriebs zur Gestaltung neuer Antriebs- und Fahrzeugarchitekturen. In *VDI – Wissensforum, Berechnung und Erprobung bei alternative Antrieben*. Baden-Baden.
- Pruckner, A., Kaspar, S., Stroph, R., and Grote, C. (2011). Vehicle dynamics per software - potentials of an electric single wheel drive. In *Proc. Conference on Future Automotive Technology, Focus Electromobility*.